

This discussion paper is/has been under review for the journal Atmospheric Chemistry and Physics (ACP). Please refer to the corresponding final paper in ACP if available.

# High resolution mapping of combustion processes and implications for CO<sub>2</sub> emissions

R. Wang<sup>1</sup>, S. Tao<sup>1</sup>, P. Ciais<sup>2,3</sup>, H. Z. Shen<sup>1</sup>, Y. Huang<sup>1</sup>, H. Chen<sup>1</sup>, G. F. Shen<sup>1</sup>,  
B. Wang<sup>1</sup>, W. Li<sup>1</sup>, Y. Y. Zhang<sup>1</sup>, Y. Lu<sup>1</sup>, D. Zhu<sup>1</sup>, Y. C. Chen<sup>1</sup>, X. P. Liu<sup>1</sup>,  
W. T. Wang<sup>1</sup>, X. L. Wang<sup>1</sup>, W. X. Liu<sup>1</sup>, B. G. Li<sup>1</sup>, and S. L. Piao<sup>1</sup>

<sup>1</sup>Laboratory for Earth Surface Processes, College of Urban and Environmental Sciences, Peking University, Beijing 100871, China

<sup>2</sup>Sino-French Institute for Earth System Science, Peking University, Beijing 100871, China

<sup>3</sup>Laboratoire des Sciences du Climat et de l'Environnement, CEA CNRS UVSQ, 91191 Gif sur Yvette, France

Received: 28 May 2012 – Accepted: 6 August 2012 – Published: 21 August 2012

Correspondence to: S. Tao (taos@pku.edu.cn)

Published by Copernicus Publications on behalf of the European Geosciences Union.

## High resolution mapping of combustion processes

R. Wang et al.

Title Page

Abstract

Introduction

Conclusions

References

Tables

Figures

⏪

⏩

◀

▶

Back

Close

Full Screen / Esc

Printer-friendly Version

Interactive Discussion

## Abstract

High-resolution mapping of fuel combustion and CO<sub>2</sub> emission provides valuable information for inferring terrestrial carbon balance, modeling pollutant transport, and developing mitigation strategies. Previous inventories included only a limited number of fuel types and anthropogenic emissions were mapped using national population proxies which may distort the geographical distribution within countries. In this study, a sub-national disaggregation method (SDM) was applied to establish a global 0.1° × 0.1° geo-referenced inventory of fuel combustion (PKU-FUEL) and a corresponding CO<sub>2</sub> emission inventory (PKU-CO<sub>2</sub>) based upon 64 fuel sub-types for the year 2007. Uncertainties of the new inventories were evaluated using a Monte Carlo method. The total combustion CO<sub>2</sub> emission in 2007 was 11.2 (9.11 and 13.3 as 5th and 95th percentiles) Pg C yr<sup>-1</sup>. By replacing national disaggregation with sub-national disaggregation in this study, the average 95th minus 5th percentile ranges of CO<sub>2</sub> emission for all grids can be reduced from 417 to 68.2 Mg km<sup>-2</sup> yr<sup>-1</sup>, indicating a significant reduction in uncertainty, because the uneven distribution of per-capita fuel consumptions within countries has been taken into account by using the sub-national fuel consumption data directly. Significant difference in per-capita CO<sub>2</sub> emissions between urban and rural areas was found in developing nations (2.09 vs. 0.600 Mg C cap<sup>-1</sup> yr<sup>-1</sup>), but not in developed ones (3.57 vs. 3.42 Mg C cap<sup>-1</sup> yr<sup>-1</sup>), suggesting strong influence of the rapid urbanization of these countries on the carbon emission. By using the CO<sub>2</sub> emission product, a new spatial pattern of terrestrial carbon sink was derived and the impact of sub-national disaggregation is discussed.

## 1 Introduction

The combustion of carbon containing fuels emits CO<sub>2</sub> and air pollutants (BP, 2008; Solomon et al., 2007; Bond et al., 2004). To quantitatively characterize climate forcing and health impacts, global emission inventories of CO<sub>2</sub> and air pollutants have been

ACPD

12, 21211–21239, 2012

## High resolution mapping of combustion processes

R. Wang et al.

Title Page

Abstract

Introduction

Conclusions

References

Tables

Figures

⏪

⏩

◀

▶

Back

Close

Full Screen / Esc

Printer-friendly Version

Interactive Discussion



## High resolution mapping of combustion processes

R. Wang et al.

Title Page

Abstract

Introduction

Conclusions

References

Tables

Figures



Back

Close

Full Screen / Esc

Printer-friendly Version

Interactive Discussion

developed. In view of data compilation difficulties, only a few major fuel types could be considered (Andres et al., 1996; JRC/PBL, 2009; Oda and Maksvutov, 2011) and detailed sector categorization was called for by the Intergovernmental Panel on Climate Change (Solomon et al., 2007). For example, it is important for policy makers to know the quantities of CO<sub>2</sub> emitted from diesel used by industry and vehicles (Davis et al., 2010). Moreover, the emission factors (EFs; the ratio of pollutant emitted per unit of fuel burned) of pollutants can differ by orders of magnitude among fuels or facilities (Bond et al., 2004; Zhang et al., 2007). In addition to fossil fuels, information on biomass and solid waste fuels is also desirable since they are among important sources of many pollutants (Bond et al., 2004; Andreae and Merlet, 2001). Emission inventories are usually geo-referenced into gridded maps using population proxy (Bond et al., 2004; Andres et al., 1996; JRC/PBL, 2009) based on national fuel data, literally assuming that per-capita fuel consumptions ( $F_{cap}$ ) or emissions ( $E_{cap}$ ) are uniform in all grids within a country (Andres et al., 1996). This method can create a spatial bias, because  $F_{cap}$  are in reality all but uniform, especially within developing countries (Zhang et al., 2007). In this regard, sub-national fuel data are more reliable (Gurney et al., 2009). There is also a growing need for emission maps of CO<sub>2</sub> and other pollutants with finer resolution for atmospheric dispersion modeling, because errors in dispersion modeling decrease with an increase in resolution (Bocquet, 2005; Tie et al., 2010). Moreover, upcoming atmospheric CO<sub>2</sub> measurements at 10 km or finer resolutions (GOSAT, OCO-2 satellites, and regional networks), require detailed CO<sub>2</sub> emission inventories for the interpretation of observed atmospheric gradients (Yokota et al., 2009; Lauvaux et al., 2009; Pillai et al., 2010). Finally, uncertainties of CO<sub>2</sub> emission inventories have never been quantified, leading to difficulty in evaluating results of any model using them (Bocquet, 2005).

We proposed a sub-national disaggregation method (SDM) for developing global 0.1° × 0.1° inventories of fuel consumptions and CO<sub>2</sub> emissions (PKU-FUEL and PKU-CO<sub>2</sub>, Peking University Fuel and CO<sub>2</sub> Inventories) for 64 sectors for the year 2007. Sub-national fuel consumption data of the major fuel types were collected for 45 countries

(7094  $0.5^\circ \times 0.5^\circ$  grids for 36 European countries (EC-36), 7942 counties for China, Mexico, and US, 161 states/provinces for India, Brazil, Canada, Australia, Turkey, and South Africa). These sub-national units were hereafter referred to as Sub-nationally Disaggregated Units (SDUs). Sub-national data for SDUs of the 45 countries and national data for other countries were disaggregated to  $0.1^\circ \times 0.1^\circ$  grids using various proxies to generate the PKU-FUEL and PKU-CO<sub>2</sub> inventories. To show the improvement by using SDM, a mock-up inventory (Nat-CO<sub>2</sub>) was generated basing on the national fuel data and disaggregation, and compared to PKU-CO<sub>2</sub>. The PKU-CO<sub>2</sub> was also compared with another two previous inventories to evaluate the new disaggregation approach. Finally, the PKU-CO<sub>2</sub> inventory was used to study the difference in CO<sub>2</sub> emission density between urban and rural areas, and applied in an inversion modeling of terrestrial ecosystem carbon fluxes. The PKU-FUEL is ready to be used to estimate global emissions of CO, NO<sub>x</sub>, black carbon, particulate matter, mercury, and many other air tracers from combustion sources.

## 2 Data and methodology

### 2.1 Combustion sources

The PKU-FUEL and PKU-CO<sub>2</sub> were constructed around 64 fuel sub-types in 5 categories and 6 sectors (Table S1). A total of 223 countries/territories were covered and classified into developing or developed countries based on the World Bank's criteria for 2007, as shown in Table S2 (World Bank, 2010). Due to difference in data sources and data processing methods, the 64 fuel sub-types were further classified into 8 groups as (1) wildfire, (2) aviation/shipping, (3) power-stations, (4) natural gas flaring, (5) agricultural solid wastes, (6) non-organized waste incineration, (7) dung cakes, and (8) others. Generally, fuel consumed in various sectors were compiled at global/national level and further allocated to  $0.1^\circ \times 0.1^\circ$  grids using various proxies. The methodology

## High resolution mapping of combustion processes

R. Wang et al.

Title Page

Abstract

Introduction

Conclusions

References

Tables

Figures

⏪

⏩

◀

▶

Back

Close

Full Screen / Esc

Printer-friendly Version

Interactive Discussion



and data sources to compile the fuel consumption for all these sources were presented in Sect. 2.2 and 2.3.

## 2.2 Compilation of fuel consumption data

For Group 1, global  $0.5^\circ \times 0.5^\circ$  wildfire carbon emissions (van der Werf et al., 2010) were converted to fuel consumptions based on the used EFs and disaggregated to  $0.1^\circ \times 0.1^\circ$  using vegetation density generated in another dataset by Friedl et al. (2002) as a proxy. For Group 2, global fuel consumptions of aviation/shipping (IEA, 2010a; IEA, 2010b; Equasis, 2008) were allocated to  $0.1^\circ \times 0.1^\circ$  using CO emission proxies based on the other dataset (Wang et al., 2008; Eyers, 2005; JRC/PBL, 2009). For Group 3, fuel consumptions by 26 239 major power stations from CARMA (contributing 77 % of the fuels used for power generation and 40 % of the global total fossil fuel emission) were allocated to individual grid-points directly (CARMA, 2010). For Group 4, fuel consumptions by natural gas flaring were derived using a regression model (Elvidge et al., 2009) based on night-light from Defense Meteorological Satellite Program (NOAA, 2011). For Group 5, the quantities of agricultural wastes burned in individual countries (provinces in China) were derived from crop production statistics (MAC, 2008; FAO, 2010), production-to-residue ratios (Bond et al., 2004; Streets et al., 2003; Cao et al., 2005; Zhang et al., 2009; Yevich and Logan, 2003), and percentage of field burned residues (Bond et al., 2004). For Group 6, quantities of non-organized wastes combusted were from total quantities of wastes generated (UNSD, 2010) and incineration rates (Bond et al., 2004; Zhang et al., 2009). For Group 7, dung cake consumption in India was compiled (TERI, 2008) and extrapolated to 12 other South and South-east Asian countries by assuming equal per-capita consumption of that fuel. At last, consumptions of all solid wastes were disaggregated to  $0.1^\circ \times 0.1^\circ$  using a population proxy from a global  $0.8 \times 0.8 \text{ km}^2$  dataset (ORNL, 2008).

### High resolution mapping of combustion processes

R. Wang et al.

Title Page

Abstract

Introduction

Conclusions

References

Tables

Figures

⏪

⏩

◀

▶

Back

Close

Full Screen / Esc

Printer-friendly Version

Interactive Discussion



### 2.3 Sub-National Disaggregation Methods (SDM)

For all other fuel sub-types (Group 8), national fuel consumptions of EC-36 (IEA, 2010a; IEA, 2010b) were disaggregated to  $0.5^\circ \times 0.5^\circ$  grids using CO emission proxies from the European Monitoring and Evaluation Programme (CEIP, 2011); National fuel consumptions of Mexico and state fuel consumptions of US (USEIA, 2008) were disaggregated to counties using CO emission proxies (USEPA, 2006; USEPA, 2011) following the method by Gurney et al. (2009). County-level fuel consumptions in China were determined based on the provincial fuel consumption (NBS, 2008) and a set of provincial-data-based regression models (Zhang et al., 2007); state/province fuel consumptions in India, Brazil, Canada, Australia, Turkey, and South Africa were directly compiled from the literature (TERI, 2008; Statistics South Africa, 2009; Brazil Energy Ministry, 2010; TSI, 2010; Environment Canada, 2010; ABES, 2008). National fuel consumptions for countries without sub-national fuel data were from the IEA (IEA, 2010a,b) and series of energy statistics (USGS, 2010a; UNID, 2008). Finally, population proxy was applied to disaggregate fuel consumptions (the 15 197 SDUs for the 45 countries and remaining 178 countries) to  $0.1^\circ \times 0.1^\circ$  grids (ORNL, 2008). The methods of disaggregation for all these sources are presented in Table S3. For the countries with no fuel data available, a set of region-specific regression models were developed to predict their fuel consumptions based on data from other countries in the same region, as listed in Table S4. Rural population, total population, and/or gross domestic production were used as independent variables (World Bank, 2010).

In processing the sub-national data for these sectors in Group 8, an inner-interpolation approach was applied following the method developed by Gurney to get the data for 64 fuel sub-types (Gurney et al., 2009). In case that sub-national data for certain fuel sub-types are not available, it was assumed that the percentages of the specific fuel consumptions within the category (coal, petroleum, natural gas, solid wastes, and biomass) in a  $0.5^\circ \times 0.5^\circ$  grid or county/state/province equal to those of the entire country. Therefore, the consumptions of the fuel sub-types in the  $0.5^\circ \times 0.5^\circ$  grids

## High resolution mapping of combustion processes

R. Wang et al.

Title Page

Abstract

Introduction

Conclusions

References

Tables

Figures



Back

Close

Full Screen / Esc

Printer-friendly Version

Interactive Discussion



or counties/states/provinces can be calculated based on the percentages of these sub-types in the category at national level (data for the five categories at national level are all available) and the total consumptions of the fuel categories in the  $0.5^\circ \times 0.5^\circ$  grid or county/state/province.

## 2.4 Development of PKU-CO<sub>2</sub>

Based on PKU-FUEL, CO<sub>2</sub> emissions (PKU-CO<sub>2</sub>) were calculated using CO<sub>2</sub> emission factors ( $EF_C$ ) and the combusted rates.  $EF_C$  for all combustion processes were derived as the means of all data collected from the literature. In detail, the  $EF_C$  for oil consumed in petroleum refinery were from a sectoral report (Nyboer et al., 2006), and the  $EF_C$  for oil consumed by 7 ship types and 5 types of biomass burning were collected from data in previous studies (van der Werf et al., 2010; Wang et al., 2008). For the remained fuel sub-types,  $EF_C$  were all collected from 5 reports (URS, 2003; IPCC, 1996; US Department of Energy, 2000; API, 2001; USEPA, 2008). Fixed combustion rates of 0.990, 0.980, 0.995, 0.980, 0.901, 0.887, 0.789, 0.919, and 0.901 were applied for petroleum, coal, natural gas, solid municipal and industrial waste fuel, biomass burned in the field, firewood burned in cook stoves, firewood burned in fireplaces, crop residue burned in cook stoves, and open burning of agriculture waste, respectively (Johnson et al., 2008; Lee et al., 2005; Oda et al., 2010; Zhang, et al., 2008). Although the study focused on fuel combustions, CO<sub>2</sub> emissions from cement production were also derived based on cement productions in 155 countries (USGS, 2010b) and CO<sub>2</sub> emission factors from the literature (Andres et al., 1996). Country-level CO<sub>2</sub> emissions from cement production were disaggregated to  $0.1^\circ \times 0.1^\circ$  grids using industrial coal consumption from PKU-FUEL as a proxy.

## 2.5 Evaluation of location accuracy of the power-stations

Fuel consumptions by 26 239 major power stations from CARMA (contributed 77 % of the fuels used for power generation and 40 % of the global total fossil fuel emission)

### High resolution mapping of combustion processes

R. Wang et al.

Title Page

Abstract

Introduction

Conclusions

References

Tables

Figures

⏪

⏩

◀

▶

Back

Close

Full Screen / Esc

Printer-friendly Version

Interactive Discussion



were allocated to individual grid-points (CARMA, 2010). As the most important sources in CO<sub>2</sub> emission, the positions of these power-stations were tested before being used in PKU-FUEL and PKU-CO<sub>2</sub>. The spatial locations for 350 randomly selected power stations were checked one by one in Google imagery for countries other than US, where the geo-locations had been demonstrated to be accurate (CARMA, 2010). The result was shown in Fig. S1. It was found that 87 and 98 % of the stations in China and other countries were located in the same or neighboring 0.1° × 0.1° grid-points in the CARMA list, respectively, indicating acceptable accuracy of the CARMA data for 0.1° × 0.1° resolution mapping. Therefore, the 0.1° × 0.1° resolution used for the PKU-FUEL and PKU-CO<sub>2</sub> does contain information spatially accurate at 0.1° and can provide better information on detailed spatial distributions of CO<sub>2</sub> than a coarser resolution. Although the CARMA is the best global power-stations dataset available up to now, the data used in allocating these power-stations is to be updated at any time when the new CARMA version product is published or a new dataset is available.

## 2.6 Monte Carlo simulations

For the Monte Carlo ensemble simulations, both PKU-FUEL and PKU-CO<sub>2</sub> were calculated 1000 times on all grids by randomly varying input data from given distributions with assumed coefficients of variation (CVs) using the disaggregation system. CVs of fuel consumptions from ships/aviation and wildfire were set to be 20 and 18 %, respectively, with normal distributions (van der Werf et al., 2010; Wang et al., 2008). A CV of 10 % was adopted for all other fuel consumptions, with a uniform distribution (Ciais et al., 2010). To consider the uncertainty associated with the spatial disaggregation of fuel data, a CV was defined for each SDU (with sub-national data) or country (without sub-national data) according to their size, with  $CV_i = 1000\% \times N_i / 225829$ , where  $N_i$  is the number of grid-points in the  $i$ -th SDU/country and 225 829 is the number of grid-points in Asian Russia, the largest SDU/country in the world, to which a CV of 1000 % was assigned. In PKU-CO<sub>2</sub>, the CVs of the literature reported  $EF_C$  range from 3.8 to 5.1 %, and thus a constant value of 5 % was adopted with normal distributions, while

## High resolution mapping of combustion processes

R. Wang et al.

Title Page

Abstract

Introduction

Conclusions

References

Tables

Figures

⏪

⏩

◀

▶

Back

Close

Full Screen / Esc

Printer-friendly Version

Interactive Discussion



the CVs of uncombusted rates were set to be 20% with a normal distribution. The results are presented using  $R_{90}$  metrics (95th minus 5th percentile range) and  $R_{90}/M$  ( $R_{90}/\text{median}$ ) for absolute and relative errors, respectively.

## 2.7 Urban-rural contrast

For each country, a population density threshold value was defined to classify urban and rural areas based on the degree of urbanization (World Bank, 2010) and the spatial distribution of population density in 2007 (ORNL, 2008). The sensitivity of the result on the threshold value was tested by re-calculating  $E_{\text{cap}}$  of urban and rural areas with the threshold value multiplied by a factor varied from 0.8 to 1.2 at a 0.1 interval. It was found that with a  $\pm 10\%$  change in the threshold, the calculated  $E_{\text{cap}}$  changed only by 0.3–0.5% (resp. 0.4–1.2%) in rural areas and by 5.5–5.8% (resp. 0.6–0.8%) in urban areas for developing (resp. developed) countries, demonstrating that the classification method is quite robust (Fig. S2). Variation in the threshold (10%, uniform distribution) was included in uncertainty characterization of urban and rural  $E_{\text{cap}}$  calculation.

## 2.8 Carbon balance of terrestrial ecosystem

For the inverse modeling, the spatial distribution of the terrestrial ecosystem  $\text{CO}_2$  fluxes,  $B(x)$  where  $x$  denotes the space coordinate, can be calculated by subtracting fossil fuel  $\text{CO}_2$  emissions,  $F(x)$ , from the net land-atmosphere  $\text{CO}_2$  fluxes distribution,  $N(x)$  (NOAA, 2010). The result of CarbonTracker inversion was used to define  $N(x)$  in 2007 (Peters et al., 2007). Two sets (i.e. maps) of  $B(x)$  were deduced as  $B(x) = N(x) - F(x)$ , with  $F(x)$  from either the PKU- $\text{CO}_2$  or NAT- $\text{CO}_2$  (downscaled to  $1^\circ \times 1^\circ$  to match the resolution of CarbonTracker). The difference between the two sets of  $B(x)$  was calculated to illustrate the effect of using the sub-national instead of national fuel data on terrestrial carbon fluxes. Explicit use of  $F(x)$  and its error structure in an atmospheric inversion is recommended in future study.

### High resolution mapping of combustion processes

R. Wang et al.

Title Page

Abstract

Introduction

Conclusions

References

Tables

Figures

⏪

⏩

◀

▶

Back

Close

Full Screen / Esc

Printer-friendly Version

Interactive Discussion

### 3 Results

#### 3.1 Global fuel consumption and CO<sub>2</sub> emission map in 2007

According to PKU-FUEL, global consumption of coal, oil, natural gas, biomass, and solid waste fuels in 2007 was 133, 154, 124, 114, and 3.59 EJyr<sup>-1</sup>, respectively. Globally,  $F_{\text{cap}}$  was 0.0733 TJcap<sup>-1</sup> yr<sup>-1</sup>, with 0.0650, 0.00829, and 0.000611 TJcap<sup>-1</sup> yr<sup>-1</sup> for fossil, anthropogenic biomass, and solid waste fuels, respectively. Mean  $F_{\text{cap}}$  for fossil fuels in developed countries (0.172 TJcap<sup>-1</sup> yr<sup>-1</sup>) was approximately 4 times of that of developing countries (0.0414 TJcap<sup>-1</sup> yr<sup>-1</sup>).

The PKU-CO<sub>2</sub> was developed based on the PKU-FUEL using CO<sub>2</sub> EFs, and combustion rates of various fuel types. Global CO<sub>2</sub> emission from all combustion sources was 11.2 PgCyr<sup>-1</sup> in 2007. Energy production, industry, residential/commercial, transportation, agriculture, and wildfires contributed 33.8, 18.0, 14.8, 15.2, 2.1, and 16.1 % of the total, respectively. Fossil, biomass, and solid waste fuels emitted 7.83, 3.18, and 0.224 PgCyr<sup>-1</sup>, respectively. The estimated fossil fuel emission (7.83 PgCyr<sup>-1</sup>) is similar to the 7.87 PgC reported by IEA (IEA, 2010c), but lower than the 9.06 PgC from EIA (USEIA, 2010), in which non-fuel-use oil products were included. The global  $E_{\text{cap}}$  from anthropogenic fuel combustion was 1.51 MgC cap<sup>-1</sup> yr<sup>-1</sup>, with large variations among and within countries. For example,  $E_{\text{cap}}$  were 0.661 and 5.74 MgC cap<sup>-1</sup> yr<sup>-1</sup> for India and US, respectively. Of the 2373 counties in China,  $E_{\text{cap}}$  varied dramatically from 0.05 to 41.1 MgC cap<sup>-1</sup> yr<sup>-1</sup>, confirming the necessity of the sub-national disaggregation approach. Emissions from individual fuel sub-types are listed in Table S5. Although this study is focused on fuel combustion, CO<sub>2</sub> emissions from cement production (0.38 PgCyr<sup>-1</sup>) were also derived to provide a more complete picture of global CO<sub>2</sub> emission. Figure 1 shows the geographical distributions of CO<sub>2</sub> emissions and  $E_{\text{cap}}$  together with the relative contributions of the 6 sectors in 9 regions as labeled pies. Regionally, power generation was the most important sector in North America (38.6%), Western Europe (46.7%), and East Asia (50.0%), while savanna burning

## High resolution mapping of combustion processes

R. Wang et al.

Title Page

Abstract

Introduction

Conclusions

References

Tables

Figures

⏪

⏩

◀

▶

Back

Close

Full Screen / Esc

Printer-friendly Version

Interactive Discussion



dominated in Africa (62.5%), South America (59.6%), and Oceania (40.9%). Emission from motor vehicles was the second largest contributor in North America (28.3%) and Western Europe (16.7%). CO<sub>2</sub> emission maps separated for the major fuel categories and sectors are shown in Fig. S3. Information on both sectoral and regional CO<sub>2</sub> emissions are presented in Table S6, which are valuable for emission prediction and regional mitigation policy formation.

### 3.2 The advantage of the PKU-CO<sub>2</sub> over the nationally disaggregated inventory (NAT-CO<sub>2</sub>)

To quantify the improvement expected in the PKU-CO<sub>2</sub>, a mock-up emission inventory (NAT-CO<sub>2</sub>, excluding point (power stations/natural gas flaring) and non-country-specific sources (aviation/shipping and wildfires)) was established using exactly the same method except that nationally aggregated fuel data and proxies were applied for the 45 countries. Emissions calculated in the SDUs of the 45 countries were compared between the PKU-CO<sub>2</sub> and NAT-CO<sub>2</sub> by calculating a relative difference criteria defined as  $RD = (E_1 - E_2) / ((E_1 + E_2) / 2)$ , where  $E_1$  and  $E_2$  are emissions in each SDU from the PKU-CO<sub>2</sub> and NAT-CO<sub>2</sub>, respectively.  $E_1$  are referred to as the More Accurate Values (MAVs), since they are directly derived from actual fuel data in each SDU without any proxy and disaggregation error. By comparison,  $E_2$  originated from national data are associated with geographic bias induced by the disaggregation to smaller scale. In another word, the RD is a metrics of the reduced bias by using sub-national disaggregation to take the  $E_{cap}$  variation among the SDUs into account. The larger the RD value, the more realistic the PKU-CO<sub>2</sub> is over the NAT-CO<sub>2</sub>.

The 45 countries with sub-national fuel data available represented 45, 61, and 69% of the global total area, population, and fuel consumption, respectively. Within these countries, CO<sub>2</sub> emissions were computed from the actual fuel data of 15 197 SDUs instead of from the national fuel data like former studies (Andres et al., 1996; Oda and Maksyutov, 2011). Although residual errors still occurred when disaggregating the emissions from SDUs to the 0.1° × 0.1° grids of the PKU-CO<sub>2</sub> product, these errors

## High resolution mapping of combustion processes

R. Wang et al.

Title Page

Abstract

Introduction

Conclusions

References

Tables

Figures



Back

Close

Full Screen / Esc

Printer-friendly Version

Interactive Discussion



should be much smaller than the errors induced by disaggregating the emissions from a country's total to  $0.1^\circ \times 0.1^\circ$  grids of the NAT-CO<sub>2</sub>. In fact, the average area of all SDUs was only 4560 km<sup>2</sup>, compared to 1 330 108 km<sup>2</sup> of the 45 countries, leading to a significantly reduction of spatial bias in the CO<sub>2</sub> emission distribution. Figure 2 shows the spatial distribution of the emission RDs for the 15 197 SDUs between the more accurate PKU-CO<sub>2</sub> and the more biased NAT-CO<sub>2</sub> emission maps. In the 9 countries with county or state/provincial data available, the country-average of the absolute RD values in all SDUs range from 17.5 (Australia) to 79.8 % (Mexico). These large RDs indicate that a substantial reduction of the spatial bias of CO<sub>2</sub> emission can be achieved by using sub-national data. It was also found that the degree of the spatial bias reduction is larger in countries with higher  $F_{cap}$  heterogeneity (e.g. large developing countries) or smaller SDUs (e.g. countries with county data).

### 3.3 Uncertainty of the PKU-CO<sub>2</sub>

Monte Carlo simulations were applied to address the uncertainties associated with data sources and disaggregation process. According to the simulation, the  $R_{90}$  for the global total CO<sub>2</sub> emission was 4.19 (range 9.11–13.3) PgCyr<sup>-1</sup> (see Table S5 for  $R_{90}$  of the 64 fuel sub-types). For the spatial distribution of CO<sub>2</sub> emissions, the absolute and relative uncertainties ( $R_{90}$  and  $R_{90}/M$ ) are mapped respectively in Fig. 3. Mean  $R_{90}$  and  $R_{90}/M$  of gridded emissions for the 45 sub-nationally disaggregated countries were 68.2 Mg km<sup>-2</sup> yr<sup>-1</sup> and 64.8 %, respectively for the PKU-CO<sub>2</sub>, compared to 417 Mg km<sup>-2</sup> yr<sup>-1</sup> and 364 % for the NAT-CO<sub>2</sub>, demonstrating a substantial reduction in the uncertainty by using SDM. However, relatively high  $R_{90}$  can be found either in large countries where sub-national fuel data are not available, such as Indonesia and Pakistan, or in areas with high emission densities such as Northern China and Western Europe.

## High resolution mapping of combustion processes

R. Wang et al.

Title Page

Abstract

Introduction

Conclusions

References

Tables

Figures

⏪

⏩

◀

▶

Back

Close

Full Screen / Esc

Printer-friendly Version

Interactive Discussion



### 3.4 Comparison with two recent inventories: ODIAC and VULCAN

The PKU-CO<sub>2</sub> map was compared with that of the ODIAC inventory (global fossil fuel, 2007, satellite nightlight-based, 1 km × 1 km, converted to 0.1° × 0.1° for the comparison) (Oda and Maksyutov, 2011) (Fig. 4). Difference in spatial pattern between the two inventories is remarkable, with ODIAC concentrating emissions more over urbanized regions. Although correlation between urban lighting and CO<sub>2</sub> emission has been demonstrated (Raupach et al., 2010; Oda et al., 2010), such a relationship is very likely to break down over populated or industrialized rural areas. For example, the strong CO<sub>2</sub> emissions from rural settlements with high population density in Sichuan, China identified in the PKU-CO<sub>2</sub> could not be detected by the satellite nightlights. Similarly, a highly-emitting coking industrial zone in Qin county, China was associated with negligible nightlight signals (the insets of Fig. 4). The underestimation of rural CO<sub>2</sub> emissions using nightlight spatialization has been indicated by Oda et al. (2010). For a comparison, RDs were calculated for all SDUs of the 45 sub-nationally disaggregated countries based on the PKU-CO<sub>2</sub> and ODIAC, and  $E_1$  (from the PKU-CO<sub>2</sub>) is considered to be the MAV. The means and standard deviations of the absolute RDs are  $113 \pm 67.3\%$  for all SDUs and range from  $28.7 \pm 29.2$  (8 SDUs in Australia) to  $116.7 \pm 67.6\%$  (2373 SDUs in China) for individual countries.

The second inventory to which PKU-CO<sub>2</sub> was compared is VULCAN, a 0.1° × 0.1° and 1 h resolution CO<sub>2</sub> emission inventory (2002, fossil fuel) established over US territory (Gurney et al., 2009). As one of the best emission products, the VULCAN is more likely to be closer to the true emissions than the PKU-CO<sub>2</sub> because it uses a large number of sectoral “process-based” data, which are not available at global scale. This is the reason why we developed the top-down sub-national disaggregation approach. After normalization (at county level to correct for the difference between 2002 and 2007), the PKU-CO<sub>2</sub> was compared to the VULCAN over US (Fig. 5). RD was calculated for each 0.1° grid-point with no MAV assumed, since both inventories are based on county fuel data. The symmetrically distributed differences are less than a factor of 2 for 68.3 % of

## High resolution mapping of combustion processes

R. Wang et al.

Title Page

Abstract

Introduction

Conclusions

References

Tables

Figures



Back

Close

Full Screen / Esc

Printer-friendly Version

Interactive Discussion



emissions, suggesting reasonable agreement and no systematic skew. The localized differences are mainly due to: (1) detailed traffic data used in the VULCAN were not available to the PKU-CO<sub>2</sub> and (2) area sources were uniformly allocated within counties in the VULCAN, but were disaggregated using population proxy in the PKU-CO<sub>2</sub>.

## 4 Discussion

### 4.1 Difference between urban and rural areas

Substantially uneven development of urban and rural areas is a key reason for  $E_{\text{cap}}$  variations within developing countries. It is interesting to compare  $E_{\text{cap}}$  between urban and rural areas, using sub-nationally spatialized data. As shown in Fig. 6, global fossil fuel  $E_{\text{cap}}$  of urban and rural areas are mapped separately, together with  $M$  and  $R_{90}$  for representative countries. Globally,  $M$  of  $E_{\text{cap}}$  were 2.45 and 0.795 MgCcap<sup>-1</sup>yr<sup>-1</sup> for urban and rural areas, respectively. The gap between rural and urban  $E_{\text{cap}}$  is large in developing countries (2.09 vs. 0.600 MgCcap<sup>-1</sup>yr<sup>-1</sup>), but small in developed countries (3.57 vs. 3.42 MgCcap<sup>-1</sup>yr<sup>-1</sup>). For the developing countries in transition (IMF, 2000),  $E_{\text{cap}}$  in urban areas were close to those of developed countries, whereas  $E_{\text{cap}}$  in rural areas were not much different from those of other developing countries. As a typical example,  $E_{\text{cap}}$  in China were 3.22 and 0.698 MgCcap<sup>-1</sup>yr<sup>-1</sup> in urban and rural areas, respectively.

The large urban-rural  $E_{\text{cap}}$  difference in developing countries is due to disparities in socioeconomic development (Dhakai, 2010; Satterthwaite, 2009). Such a difference is a key driver of future emission trends and should be addressed when formulating carbon mitigation policy. For example, China has experienced a rapid urbanization with urban population grew up from 19.6% in 1980 to 42.2% in 2007 (World Bank, 2010). A substantial change in economic activity and life style of the new urban settlers was very likely associated with the 3.2 times increase in country's  $E_{\text{cap}}$  (IEA, 2010c). It is anticipated that a rapid increase in CO<sub>2</sub> emissions due to the fact that millions of people

## High resolution mapping of combustion processes

R. Wang et al.

Title Page

Abstract

Introduction

Conclusions

References

Tables

Figures

⏪

⏩

◀

▶

Back

Close

Full Screen / Esc

Printer-friendly Version

Interactive Discussion



will continue to migrate from rural to urban areas in developing countries is inevitable. Changes in the energy structure in rural areas of developing countries is also taking place with improved stoves, biogas, liquid petroleum gas, and electric appliances being used increasingly (Cai and Jiang, 2008). Although this trend could improve energy efficiency and reduce emissions of air pollutants, the replacement of traditional biomass fuels by fossil fuels and electricity may result in greater net CO<sub>2</sub> flux (Solomon et al., 2007).

## 4.2 Application to inversion modeling of terrestrial ecosystem CO<sub>2</sub> fluxes

Terrestrial ecosystems have acted as a carbon sink (Houghton, 2007). However, the spatial distribution of this sink inferred using atmospheric CO<sub>2</sub> measurements and inverse modeling method remains elusive, partly due to the lack of emission information with high spatial and temporal resolutions (Lauvaux et al., 2009). By reducing the uncertainty in spatial distribution of CO<sub>2</sub> emissions, an inventory like the PKU-CO<sub>2</sub> helps to reduce uncertainty in atmospheric inverse modeling, which infers terrestrial carbon fluxes as the difference between net CO<sub>2</sub> land-atmosphere fluxes (calculated from stations CO<sub>2</sub> data and transport modeling) and the (assumed to be well known) fossil fuel CO<sub>2</sub> emissions. To do so, the PKU-CO<sub>2</sub> and NAT-CO<sub>2</sub> are compared for deducing the carbon flux of terrestrial ecosystems using CarbonTracker inverse model output for 2007 (NOAA, 2010). The calculated terrestrial ecosystem CO<sub>2</sub> fluxes,  $B(x)$  (see the Methods section), based on the CarbonTracker inversion (NOAA, 2010) and the PKU-CO<sub>2</sub> emission product is shown in Fig. 7. With the more accurate PKU-CO<sub>2</sub> emission inventory subtracted from the CarbonTracker net CO<sub>2</sub> flux, a new pattern of terrestrial CO<sub>2</sub> sources and sinks is obtained, which was different with the original result (NOAA, 2010). To test the effect of sub-national disaggregation of emissions on  $B(x)$  distribution, differences in the  $B(x)$  calculated based on the PKU-CO<sub>2</sub> and NAT-CO<sub>2</sub> are mapped in Fig. 7. The mean absolute differences in  $B(x)$  were 40.5, 52.1, 28.2, 17.9, 3.05, and 0.695 gC km<sup>-2</sup> yr<sup>-1</sup> for all grids in China, Mexico, US, India, Brazil, and Australia, respectively.

## High resolution mapping of combustion processes

R. Wang et al.

Title Page

Abstract

Introduction

Conclusions

References

Tables

Figures



Back

Close

Full Screen / Esc

Printer-friendly Version

Interactive Discussion



## 5 Conclusions

The PKU-FUEL and PKU-CO<sub>2</sub> are the first global sub-nationally disaggregated 0.1° × 0.1° carbon-fuel combustion and CO<sub>2</sub> emission inventories with 64 fuel sub-types and uncertainty assessments. The major improvements of PKU-CO<sub>2</sub> over previous inventories are (1) a large database of sub-national fuel consumptions was compiled and used for 45 major countries, which explicitly accounts for uneven distributions of  $F_{\text{cap}}$  and  $E_{\text{cap}}$  within these countries; (2) fossil, biomass, and solid waste fuels were included and categorized into 64 sub-types in 6 economic sectors, to provide detailed source information; and (3) uncertainties of the inventories were quantified. As a result, relative uncertainty range ( $R_{90}/M$ ) of CO<sub>2</sub> emission could be reduced from 364 to 64.8 % by using the sub-national disaggregation. In the 9 countries with sub-national data of different level available, the distortion by using nationally disaggregation method can be reduced by 17.5 ~ 79.8 %, indicating a substantial reduction of the spatial bias of CO<sub>2</sub> emission. It was also found that the degree of the spatial bias reduction is larger in countries with higher degree of unbalance or with smaller SDUs applied.

The inventory can be further improved by compiling more sub-national fuel consumption data for other large countries. Inventories with temporal resolutions, both intra- and inter-annual, are also needed. The significant difference in CO<sub>2</sub> emissions between urban and rural areas in transition countries suggests that more studies on the effect of rapid urbanization on CO<sub>2</sub> emissions should be addressed. The PKU-FUEL is ready to be used for estimating emissions of other greenhouse gases, black carbon, and various air pollutants, which can help us to improve the understanding on combustion-related climate forcing and health impact.

**Supplementary material related to this article is available online at:**  
**[http://www.atmos-chem-phys-discuss.net/12/21211/2012/  
acpd-12-21211-2012-supplement.zip](http://www.atmos-chem-phys-discuss.net/12/21211/2012/acpd-12-21211-2012-supplement.zip)**

### High resolution mapping of combustion processes

R. Wang et al.

Title Page

Abstract

Introduction

Conclusions

References

Tables

Figures



Back

Close

Full Screen / Esc

Printer-friendly Version

Interactive Discussion



*Acknowledgements.* Funding for this study was provided by the National Natural Science Foundation of China (41130754). CarbonTracker 2010 results were provided by NOAA ESRL, Boulder, Colorado, USA (<http://carbontracker.noaa.gov>). We thank Tomohiro Oda (NOAA Earth System Research Lab) and Shamil Maksyutov (National Institute for Environmental Studies, Japan) for providing the original data of ODIAC and valuable comments, Christopher D. Elvidge (NOAA National Geophysical Data Center) for helping us to retrieve natural gas flaring data, and Brian Reid (University of East Anglia) for valuable comments and proof reading.

## References

- American Petroleum Institute (API): Compendium of Greenhouse Gas Emissions Estimation Methodologies for the Oil and Gas Industry, Pilot Test Version, available at: <http://www.global.ihf.com>, 2001.
- Andreae, M. O. and Merlet, P.: Emission of trace gases and aerosols from biomass burning, *Global Biogeochem. Cy.*, 15, 955–966, 2001.
- Andres, R. J., Marland, G., Fung, I. E., and Matthews, E. A.:  $1^\circ \times 1^\circ$  distribution of carbon dioxide emissions from fossil fuel consumption and cement manufacture, 1950–1990, *Global Biogeochem. Cy.*, 10, 419–429, 1996.
- Australian Bureau of Agricultural and Resource Economics and Sciences (ABARES): Energy in Australia 2008, available at: <http://www.abares.gov.au/publications>, 2008.
- Bocquet, M.: Grid resolution dependence in the reconstruction of an atmospheric tracer source, *Nonlinear Proc. Geophys.*, 34, 521–529, 2005.
- Bond, T. C., Streets, D. G., Fernandes, S. D., Nelson, S. M., Yarber, K. F., Woo, J.-H., and Klimont, Z.: A technology-based global inventory of black and organic carbon emissions from combustion, *J. Geophys. Res. Atmos.*, 109, D14203, 2004.
- Brazil Energy Ministry: Brazil Energy Statistics, available at: <http://www.mme.gov.br/mme>, 2010.
- British Petroleum (BP): Statistical Review of World Energy-2007, available at: <http://www.bp.com>, 2008.
- Cai, J. and Jiang, Z.: Changing of energy consumption patterns from rural households to urban households in China: an example from Shaanxi Province, China, *Renew. Sust. Energ. Rev.*, 12, 1667–1680, 2008.

## High resolution mapping of combustion processes

R. Wang et al.

Title Page

Abstract

Introduction

Conclusions

References

Tables

Figures



Back

Close

Full Screen / Esc

Printer-friendly Version

Interactive Discussion



## High resolution mapping of combustion processes

R. Wang et al.

Title Page

Abstract

Introduction

Conclusions

References

Tables

Figures

⏪

⏩

◀

▶

Back

Close

Full Screen / Esc

Printer-friendly Version

Interactive Discussion



- Cao, G. L., Zhang, X. Y., Wang, D., and Zheng, F. C.: Inventory of emissions of pollutants from open burning crop biomass, *J. Agr. Environ. Sci.* 24, 800–804, 2005.
- CARMA: <http://www.CARMA.org>, last access: 1 Dec 2012, 2010.
- Centre on Emission Inventories and Projections (CEIP): Emissions as used in EMEP models, available at: <http://www.ceip.at> (last access: 14 August 2012), 2011.
- Ciais, P., Paris, J. D., Marland, G., Peylin, P., Piao, S. L., Levin, I., Pregger, T., Scholz, Y., Friedrich, R., Rivier, L., Houwelling, S., Schulze, E. D., and members of the CARBOEUROPE SYNTHESIS TEAM (1): The European carbon balance. Part 1: fossil fuel emissions, *Global Change Biol.*, 16, 1395–1408, 2010.
- Davis, S. J., Caldeira, K., and Matthews, H. D.: Future CO<sub>2</sub> emissions and climate change from existing energy infrastructure, *Science*, 329, 1330–1332, 2010.
- Dhokal, S. GHG emissions from urbanization and opportunities for urban carbon mitigation, *Curr. Opin. Env. Sust.*, 2, 277–283, 2010.
- Elvidge, C. D., Ziskin, D., Baugh, K. E., Tuttle, B. T., Ghosh, T., Pack, D. W., Erwin, E. H., and Zhizhin, M.: A fifteen year record of global natural gas flaring derived from satellite data, *Energies*, 2, 595–622, 2009.
- Environment Canada/Natural Resource Canada: State Energy Statistics 2007, available at: [www.nrcan.gc.ca](http://www.nrcan.gc.ca), 2010.
- Equasis: The world merchant fleet in 2007 (Lisbon), available at: <http://www.equasis.org/EquasisWeb/public/HomePage> (last access: 14 August 2012), 2008.
- European Commission, Joint Research Centre (JRC)/Netherlands Environmental Assessment Agency (PBL): Emission Database for Global Atmospheric Research (EDGAR), version 4.0., Netherland, available at: <http://edgar.jrc.ec.europa.eu>, 2009.
- Eyers, V., Kohler, H. W., van Aardenne, J., and Lauer, A.: Emissions from international shipping: 1. The last 50 years, *J. Geophys. Res.*, 110, D17305, 2005.
- Food and Agriculture Organization of the United Nations (FAO): FAOSTAT food and agriculture statistics, available at: <http://faostat.fao.org/default.aspx>, 2010.
- Friedl, M. A., McIver, D. K., Hodges, J., Zhang, X. Y., Muchoney, D., Strahler, A. H., Woodcock, C. E., Gopal, S., Schneider, A., Cooper, A., Baccini, A., Gao, F., and Schaaf, C.: Global 10 land cover mapping from MODIS: algorithms and early results, *Remote Sens. Environ.*, 83, 287–302, 2002.

## High resolution mapping of combustion processes

R. Wang et al.

Title Page

Abstract

Introduction

Conclusions

References

Tables

Figures

⏪

⏩

◀

▶

Back

Close

Full Screen / Esc

Printer-friendly Version

Interactive Discussion



Gurney, K. R., Mendoza, D. L., Zhou, Y., Fischer, M. L., Miller, C. C., Geethakumar, S., and de la Rue du Can, S.: High resolution fossil fuel combustion CO<sub>2</sub> emission fluxes for the United States, *Environ. Sci. Technol.*, 43, 5535–5541, 2009.

Houghton, R. A.: Balancing the global carbon budget, *Annu. Rev. Earth Pl. Sc.*, 35, 313–347, 2007.

Intergovernmental Panel on Climate Change (IPCC): Revised 1996 IPCC Guidelines for National Greenhouse Gas Inventories, Reference Manual (Volume 3), United Nations Environment Programme, the Organization for Economic Co-operation and Development, the International Energy Agency, IPCC, available at: <http://www.ipcc-nggip.iges.or.jp/public/gl/invs1.htm>, 1996.

International Energy Agency (IEA): Energy Statistics and Balances of Non-OECD Countries, 2007–2008, Paris, 2010a.

International Energy Agency (IEA): Energy Statistics and Balances of Non-OECD Countries, 2007–2008, Paris, 2010b.

International Energy Agency (IEA): CO<sub>2</sub> Emission From Fuel Combustion-2011 Highlights, Paris, 2010c.

International Monetary Fund (IMF): Transition Economies: An IMF Perspective on Progress and Prospects, available at: <http://www.imf.org/external/np/exr/ib/2000/110300.htm>, 2000.

Johnson, M., Edwards, R., Frenk, C. A., and Masera, O.: In-field greenhouse gas emissions from cookstoves in rural Mexican households, *Atmos. Environ.*, 42, 1206–1222, 2008.

Lauvaux, T., Pannekoucke, O., Sarrat, C., Chevallier, F., Ciais, P., Noilhan, J., and Rayner, P. J.: Structure of the transport uncertainty in mesoscale inversions of CO<sub>2</sub> sources and sinks using ensemble model simulations, *Biogeosciences*, 6, 1089–1102, doi:10.5194/bg-6-1089-2009, 2009.

Lee, S., Baumann, K., Schauer, J. J., Sheesley, R. J., Naeher, L. P., Meinardi, S., Blake, D. R., Edgerton, E. S., Russell, A. G., and Clements, M.: Gaseous and particulate emissions from prescribed burning in Georgia, *Environ. Sci. Technol.*, 39, 9049–9056, 2005.

Ministry of Agriculture of China (MAC): China Agriculture Yearbook 2008, China Agriculture Press, Beijing, 2008.

National Bureau of Statistics (NBS): China Energy Statistical Yearbook 2007, China Statistics Press, Beijing, 2008.

NOAA Earth System Research Laboratory/Global Monitoring Division: CarbonTracker 1° × 1° Land Fluxes Datasets, available at: <http://carbontracker.noaa.gov>, 2010.

## High resolution mapping of combustion processes

R. Wang et al.

Title Page

Abstract

Introduction

Conclusions

References

Tables

Figures

⏪

⏩

◀

▶

Back

Close

Full Screen / Esc

Printer-friendly Version

Interactive Discussion

- NOAA Earth Observation Group: Global Gas Flaring Estimates, available at: [http://www.ngdc.noaa.gov/dmsp/interest/gas\\_flares.html](http://www.ngdc.noaa.gov/dmsp/interest/gas_flares.html), 2011.
- Nyboer, J., Strickland, C., and Tu, J. J.: Improved CO<sub>2</sub>, CH<sub>4</sub> and N<sub>2</sub>O Emission Factors for Producer-Consumed Fuels in Oil Refinerie, Canadian Industrial End-use Energy Data and Analysis Centre, 2006.
- Oak Ridge National Laboratory (ORNL): LandScan Global Population 2007 Database, available at: <http://www.ornl.gov/sci/landscan/>, 2008.
- Oda, T. and Maksyutov, S.: A very high-resolution (1 km×1 km) global fossil fuel CO<sub>2</sub> emission inventory derived using a point source database and satellite observations of nighttime lights, *Atmos. Chem. Phys.*, 11, 543–556, doi:10.5194/acp-11-543-2011, 2011.
- Oda, T., Maksyutov, S., and Elvidge, C. D.: Disaggregation of national fossil fuel CO<sub>2</sub> emissions using a global power plant database and DMSP nightlight data, Proc. of the 30th Asia-Pacific Advanced Network Meeting, 220–229, 2010.
- Peters, W., Jacobson, A. R., Sweeney, C., Andrews, A. E., Conway, T. J., Masarie, K., Miller, J. B., Bruhwiler, L. M. P., Petron, G., Hirsch, A. I., Worthy, D. E. J., van der Werf, G. R., Randerson, J. T., Wennberg, P. O., Krol, M. C., and Tans, P. P.: An atmospheric perspective on North American carbon dioxide exchange: CarbonTracker, *P. Natl. Acad. Sci. USA*, 104, 18925–18930, 2007.
- Pillai, D., Gerbig, C., Marshall, J., Ahmadov, R., Kretschmer, R., Koch, T., and Karstens, U.: High resolution modeling of CO<sub>2</sub> over Europe: implications for representation errors of satellite retrievals, *Atmos. Chem. Phys.*, 10, 83–94, 2009, <http://www.atmos-chem-phys.net/10/83/2009/>.
- Raupach, M. R., Rayner, P. J., and Paget, M.: Regional variations in spatial structure of night-lights, population density and fossil-fuel CO<sub>2</sub> emissions, *Energ. Policy*. 38, 756–4764, 2010.
- Satterthwaite, D.: The implications of population growth and urbanization for climate change, *Environ. Urban.*, 21, 545–567, 2009.
- Solomon, S., Qin, D., Manning, M., Chen, Z., Marquis, M., Averyt, K. B., Tignor, M., and Miller, H. L.: IPCC Climate Change 2007: The Physical Science Basis, Cambridge Univ. Press, Cambridge, 2007.
- Statistics South Africa: Energy Accounts for South Africa: 2002–2006, Statistics South Africa, Pretoria, 2009.

## High resolution mapping of combustion processes

R. Wang et al.

Title Page

Abstract

Introduction

Conclusions

References

Tables

Figures

⏪

⏩

◀

▶

Back

Close

Full Screen / Esc

Printer-friendly Version

Interactive Discussion



Streets, D., Yarber, K., Woo, J. H., and Carmichael, G. R.: Biomass burning in Asia: annual and seasonal estimates and atmospheric emissions, *Global Biogeochem. Cy.*, 17, 1099, doi:10.1029/2003GB002040, 2003.

Tata Energy Research Institute (TERI): Tata Energy Directory and Data Yearbook 2007, New Delhi, India, 2008.

Tie, X., Brasseur, G., and Ying, Z.: Impact of model resolution on chemical ozone formation in Mexico City: application of the WRF-Chem model, *Atmos. Chem. Phys.*, 10, 8983–8995, 2010, <http://www.atmos-chem-phys.net/10/8983/2010/>.

Turkish Statistical Institute (TSI): Turkish Statistical Institute Regional Statistics 2007, available at: <http://tuikapp.tuik.gov.tr/Bolgesel/sorguSayfa.do?target=tablo>, 2010.

U.N. Industrial Development Organization (UNID): International Yearbook of Industrial Statistics 2008, Edward Elgar Publishing, Inc. Cheltenham, Glos GL50 1UA, UK, 2008.

US Energy Information Administration (USEIA): State Energy Data, available at: <http://www.eia.gov/>, 2008.

US Energy Information Administration (USEIA): World Carbon Dioxide Emissions from the Use of Fossil Fuels (Washington DC), available at: <http://www.eia.gov/cfapps/ipdbproject/IEDIndex3.cfm?tid=90&pid=44&aid=8>, 2010.

US Geological Survey (USGS): Aluminum Statistics and Information 2007, available at: <http://minerals.usgs.gov/minerals/pubs/commodity/aluminum/>, 2010a.

US Geological Survey (USGS): Cement Statistics and Information 2007, available at: <http://minerals.usgs.gov/minerals/pubs/commodity/cement/>, 2010b.

United Nations Statistics Division (UNSD): Environmental Indicators: Waste, available at: <http://unstats.un.org/unsd/environment/qindicators.htm>, 2010.

United States Environmental Protection Agency (USEPA): Emission factor documentation for AP-42, available at: <http://www.epa.gov/ttn/chief/ap42/index.html>, 2008.

United States Environmental Protection Agency (USEPA): Mexico national emissions inventory, available at: <http://www.epa.gov/ttn/chief/net/mexico.html>, 2006.

United States Environmental Protection Agency (USEPA): National Emissions Inventory Data & Documentation (USEPA, Research Triangle Park, NC), available at: <http://www.epa.gov/ttn/chief/net/2008inventory.html>, 2011.

URS: Corporation EME Greenhouse Gas Emission Factor Review – Final Technical Memorandum, Austin, Texas, 2003.

US Department of Energy: Instructions for Form EIA 1605 Voluntary Reporting of Greenhouse Gases, Appendix B – Fuel and Energy Source Codes and Emission Coefficients, available at: [http://www.eia.gov/oiaf/1605/reportingform\\_prelaunch.html](http://www.eia.gov/oiaf/1605/reportingform_prelaunch.html) (last access: 14 August 2012), 2000.

5 van der Werf, G. R., Randerson, J., Giglio, L., Collatz, G., Mu, M., Kasibhatla, P. S., Morton, D. C., DeFries, R. S., Jin, Y., and van Leeuwen, T. T.: Global fire emissions and the contribution of deforestation, savanna, forest, agriculture, and peat fires, *Atmos. Chem. Phys.*, 10, 16153–16230, 2010,  
<http://www.atmos-chem-phys.net/10/16153/2010/>.

10 Wang, C., Corbett, J. J., and Firestone, J.: Improving spatial representation of global ship emissions inventories, *Environ. Sci. Technol.*, 42, 193–199, 2008.

World Bank: World Development Indicators, available at: <http://databank.worldbank.org/ddp/home.do>, 2010.

15 Yevich, R. and Logan, J. A.: An assessment of biofuel use and burning of agricultural waste in the developing world, *Global Biogeochem. Cy.*, 17, 2002GB001952, 2003.

Yokota, T., Yoshida, Y., Eguchi, N., Ota, Y., Tanaka, T., Watanabe, H., and Maksyutov, S.: Global concentrations of CO<sub>2</sub> and CH<sub>4</sub> retrieved from GOSAT: first preliminary results, *SOLA*, 5, 160–163, 2009.

20 Zhang, H., Ye, X., Cheng, T., Chen, J., Yang, X., Wang, L., and Zhang, R.: A laboratory study of agricultural crop residue combustion in China: emission factors and emission inventory, *Atmos. Environ.*, 42, 8432–8441, 2008.

Zhang, Y. X. and Tao, S.: Global atmospheric emission inventory of polycyclic aromatic hydrocarbons (PAHs) for 2004, *Atmos. Environ.*, 43, 812–819, 2009.

25 Zhang, Y. X., Tao, S., Cao, J., and Coveney, R. M.: Emission of polycyclic aromatic hydrocarbons in China by county. *Environ. Sci. Technol.*, 41, 683–687, 2007.

ACPD

12, 21211–21239, 2012

## High resolution mapping of combustion processes

R. Wang et al.

Title Page

Abstract

Introduction

Conclusions

References

Tables

Figures

⏪

⏩

◀

▶

Back

Close

Full Screen / Esc

Printer-friendly Version

Interactive Discussion

High resolution mapping of combustion processes

R. Wang et al.

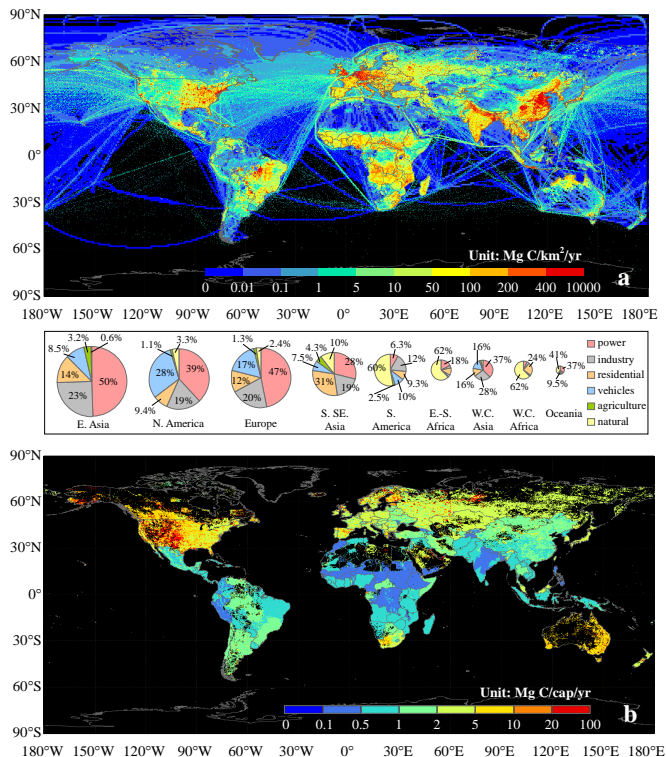


**Fig. 1.** Geographic distributions of total and per-capita CO<sub>2</sub> emissions from combustion sources at 0.1° × 0.1° resolution in 2007 from the PKU-CO<sub>2</sub> inventory developed in this study. **(a)** Total CO<sub>2</sub> emissions from all combustion sources and **(b)** per-capita anthropogenic CO<sub>2</sub> emissions excluding shipping and aviation. For total emission of each region, the relative contribution of each sector is shown in the pie charts in the inset and the total area of each pie is proportional to the emission of region considered. The emissions in North Africa and Caribbean/Central America are too small to be shown as pie charts.

Title Page

Abstract Introduction

Conclusions References

Tables Figures

⏪ ⏩

◀ ▶

Back Close

Full Screen / Esc

Printer-friendly Version

Interactive Discussion

## High resolution mapping of combustion processes

R. Wang et al.

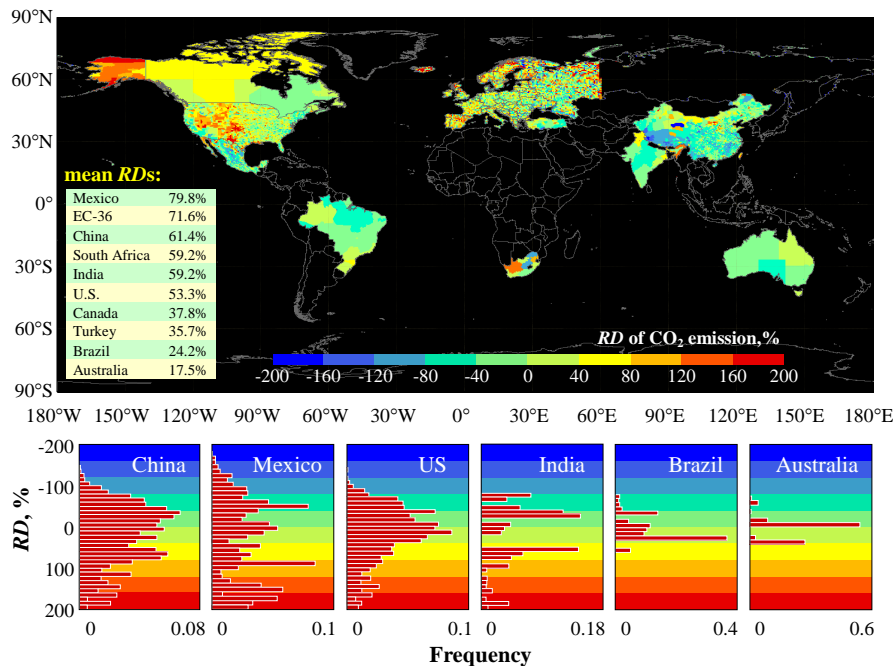


**Fig. 2.** Comparison of CO<sub>2</sub> emissions at the scale of sub-nationally disaggregated units (SDUs, e.g. counties, states/provinces, or 0.5° grids) in 45 countries between the sub-nationally (PKU-CO<sub>2</sub>) and nationally (NAT-CO<sub>2</sub>) disaggregated inventories. RDs between the PKU-CO<sub>2</sub> and NAT-CO<sub>2</sub> inventory were calculated for all SDUs with sub-national fuel consumption data specially compiled for the PKU-CO<sub>2</sub> (0.5° × 0.5° grids in EC-36, counties in China, Mexico, and US, and states/provinces in India, Brazil, Canada, Australia, Turkey, and South Africa). Mean absolute RDs for these countries are listed at the bottom-left of the map. A positive value indicates an underestimation by national data disaggregation. Frequency distributions of RDs for China, Mexico, US, India, Brazil, and Australia are shown in the bar charts at the bottom.

Title Page

Abstract Introduction

Conclusions References

Tables Figures

◀ ▶

◀ ▶

Back Close

Full Screen / Esc

Printer-friendly Version

Interactive Discussion



## High resolution mapping of combustion processes

R. Wang et al.

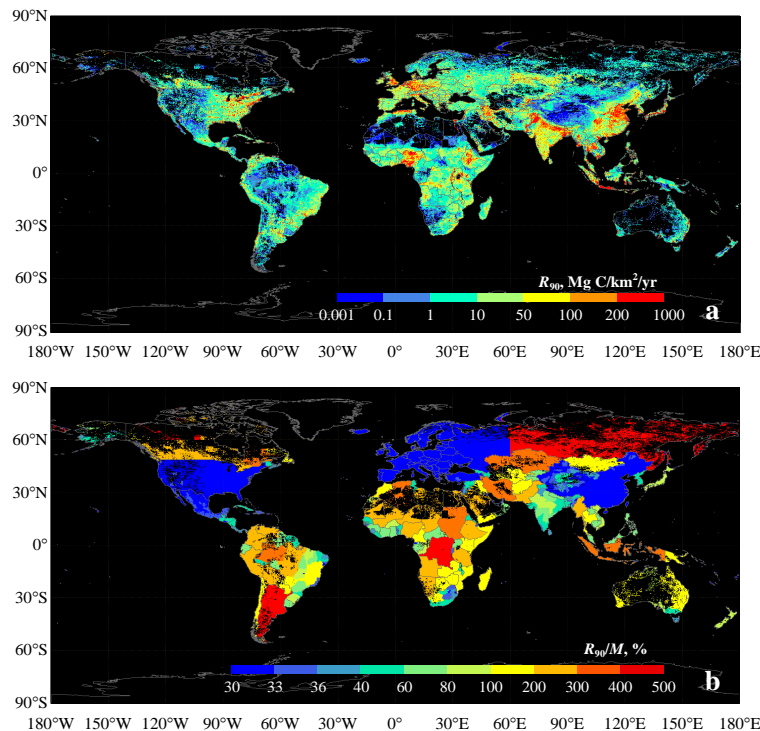


**Fig. 3.** Geographical distributions of absolute and relative uncertainties of CO<sub>2</sub> emissions from combustion sources, excluding shipping and aviation at  $0.1^\circ \times 0.1^\circ$  resolution. **(a)** Absolute uncertainties as  $R_{90}$  and **(b)** relative uncertainties as  $R_{90}/M$ , where  $R_{90}$  and  $M$  are the 95th minus 5th percentile range and median value obtained in each grid-point calculated from 1000 Monte Carlo simulations with randomly varied input data, respectively.

Title Page

Abstract

Introduction

Conclusions

References

Tables

Figures

⏪

⏩

◀

▶

Back

Close

Full Screen / Esc

Printer-friendly Version

Interactive Discussion

## High resolution mapping of combustion processes

R. Wang et al.

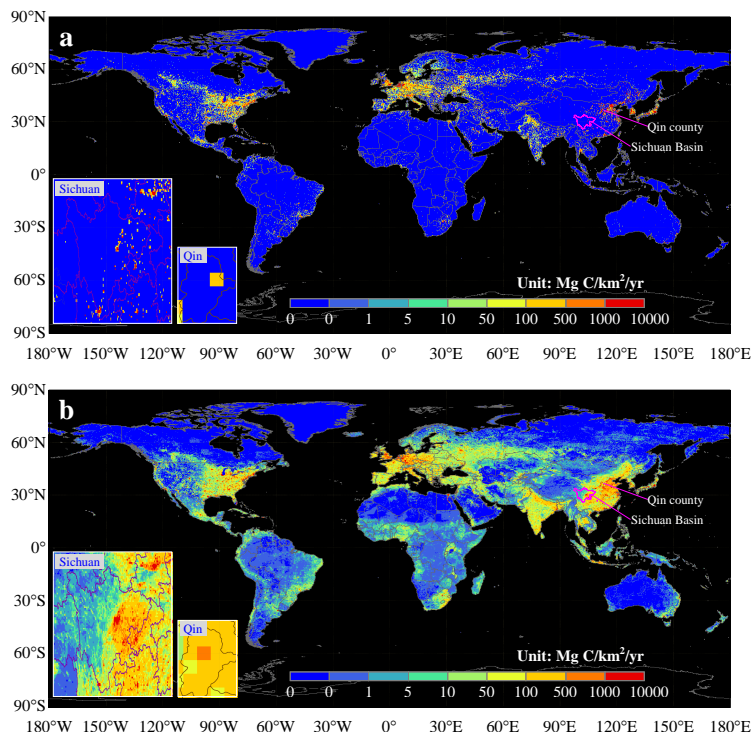


**Fig. 4.** Comparison between the ODIAC (2007) and PKU-CO<sub>2</sub> (2007) for fossil fuel emissions excluding shipping and aviation. **(a)** The ODIAC and **(b)** the PKU-CO<sub>2</sub>. Emissions in a coking industrial zone in rural area of Qin county, China and heavily populated Sichuan Basin, China are shown in the insets at the bottom-left of the maps. The grids with zero emission are filled with dark blue.

[Title Page](#)[Abstract](#)[Introduction](#)[Conclusions](#)[References](#)[Tables](#)[Figures](#)[⏪](#)[⏩](#)[⏴](#)[⏵](#)[Back](#)[Close](#)[Full Screen / Esc](#)[Printer-friendly Version](#)[Interactive Discussion](#)

## High resolution mapping of combustion processes

R. Wang et al.

Title Page

Abstract

Introduction

Conclusions

References

Tables

Figures

◀

▶

◀

▶

Back

Close

Full Screen / Esc

Printer-friendly Version

Interactive Discussion

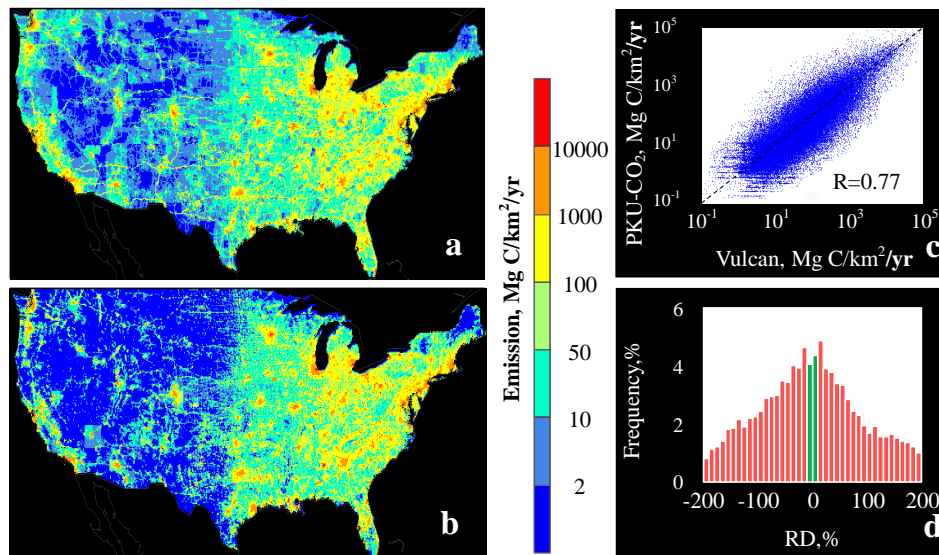


**Fig. 5.** Comparison between the VULCAN (a very detailed fossil fuel CO<sub>2</sub> emission inventory, only available over the US territory, normalized for individual counties to correct for the difference between 2002 and 2007) and the PKU-CO<sub>2</sub> inventory (this study). **(a)** The normalized VULCAN inventory; **(b)** the PKU-CO<sub>2</sub> inventory; **(c)** log-scaled plot of grid emissions (84 166 grid-points) in the PKU-CO<sub>2</sub> against those in the VULCAN; **(d)** the frequency distribution of relative differences (RD) of grid emissions between the normalized VULCAN inventory and the PKU-CO<sub>2</sub> inventory. A negative RD indicates an overestimation for the emission in the grid by the PKU-CO<sub>2</sub> inventory.

## High resolution mapping of combustion processes

R. Wang et al.

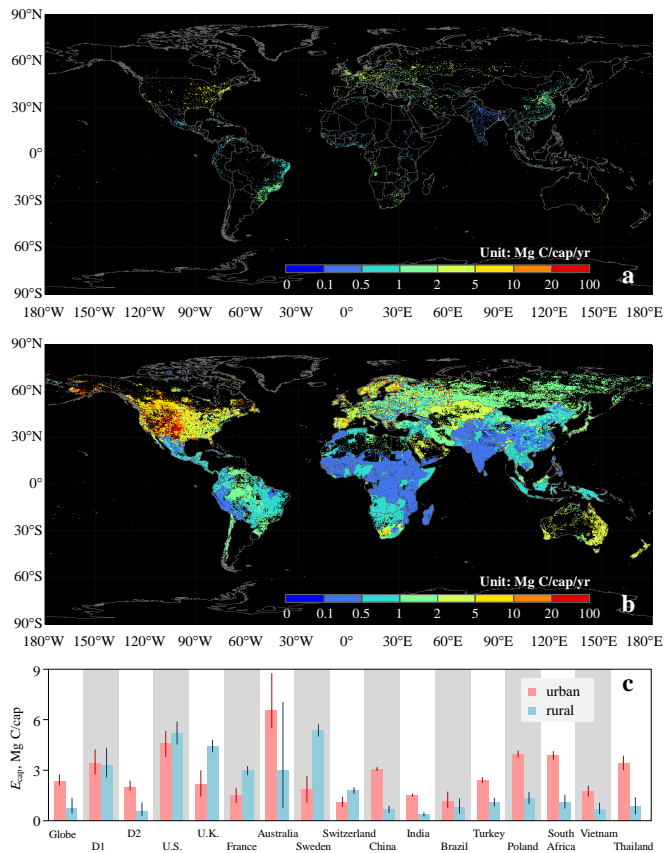


**Fig. 6.** Comparison in per-capita fossil fuel CO<sub>2</sub> emissions between urban and rural areas. **(a)** Urban  $E_{cap}$  map, **(b)** rural  $E_{cap}$  map, and **(c)**  $E_{cap}$  as  $M$  and  $R_{90}$  from the Monte Carlo simulations for 14 representative countries, all developed countries (D1), all developing countries (D2), and the globe. For the Monte Carlo simulations, both variations in the PKU-CO<sub>2</sub> and urban-rural classification criteria (uniform distribution,  $\pm 10\%$ ) were taken into consideration.

## High resolution mapping of combustion processes

R. Wang et al.

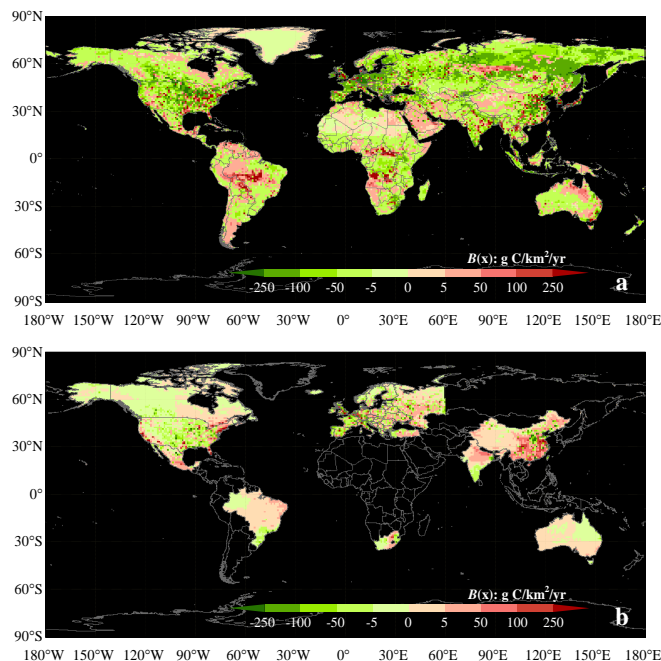


**Fig. 7.** Geographic distribution of terrestrial ecosystem carbon flux deduced by subtracting from the net land-atmosphere carbon flux in an atmospheric inversion. **(a)** Carbon balance based on the PKU-CO<sub>2</sub> emission map, and the negative (positive) values are corresponding to carbon sinks (sources), and **(b)** map of calculated differences in terrestrial ecosystem carbon fluxes in SDUs based on the PKU-CO<sub>2</sub> map and the (regionally) less accurate NAT-CO<sub>2</sub> map relying on national fuel data only for the 45 countries, and the negative (positive) values indicate that the carbon fluxes from air to surface derived from the PKU-CO<sub>2</sub> were larger (smaller) than those from the NAT-CO<sub>2</sub>. This result depends on the inversion model used and the two maps are shown only as an example.

[Title Page](#)[Abstract](#)[Introduction](#)[Conclusions](#)[References](#)[Tables](#)[Figures](#)[⏪](#)[⏩](#)[◀](#)[▶](#)[Back](#)[Close](#)[Full Screen / Esc](#)[Printer-friendly Version](#)[Interactive Discussion](#)